nature portfolio

https://doi.org/10.1038/s41586-025-09335-x

Supplementary information

Lithium deficiency and the onset of Alzheimer's disease

In the format provided by the authors and unedited

Supplementary figures

Liviu Aron, Zhen Kai Ngian, Chenxi Qiu, Jaejoon Choi, Marianna Liang, Derek M. Drake, Sara E. Hamplova, Ella Lacey, Perle Roche, Monlan Yuan, Saba S. Hazaveh, Eunjung A. Lee, David A. Bennet & Bruce A. Yankner

Lithium Deficiency and the Onset of Alzheimer's Disease

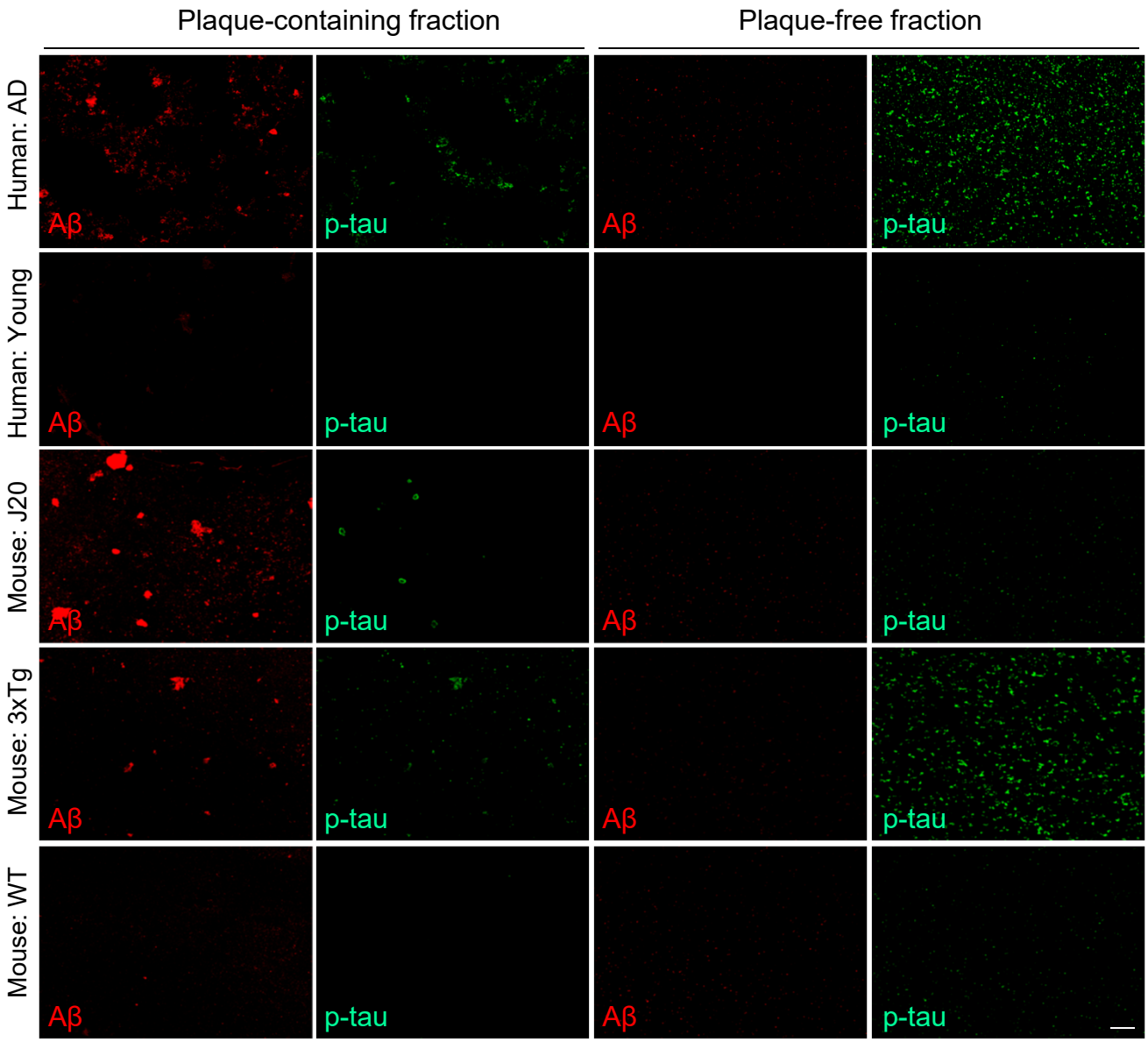

Supplementary Fig. 1. Characterization of plaque-enriched and non-plaque brain fractions. Biochemically separated plaque-enriched and non-plaque fractions were immunolabeled for Aβ and pSer202-tau (antibody CP13). Aggregated Aβ was detected in plaque-enriched fractions from human AD, J20, and 3xTg mouse cortex, but not in corresponding non-plaque fractions. In contrast, phospho-tau localized primarily to non-plaque fractions. Young adult human and WT mouse brains served as controls and showed minimal Aβ or phospho-tau accumulation. Scale bar, 50 μm.

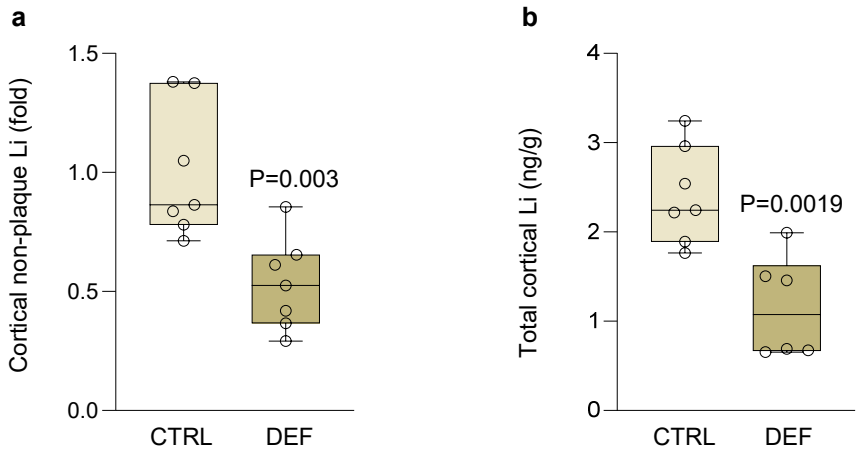

Supplementary Fig. 2. Measurement of Li levels in Li-deficient and control mice. a, Li levels in non-plaque cortical fractions of 12-month-old 3xTg mice after 5 weeks on Li-deficient (DEF, n=7) or control (CTRL, n=7) diets, normalized to CTRL. **b**, Total cortical Li levels in 12-month-old 3xTg mice after 7 months on DEF (n=6 mice) or CTRL (n=7) diets. Box plots show individual values, median (line), box limits (25^{th}-75^{th} percentiles), and whiskers (min-max). The data was analyzed by two-tailed unpaired t-test.

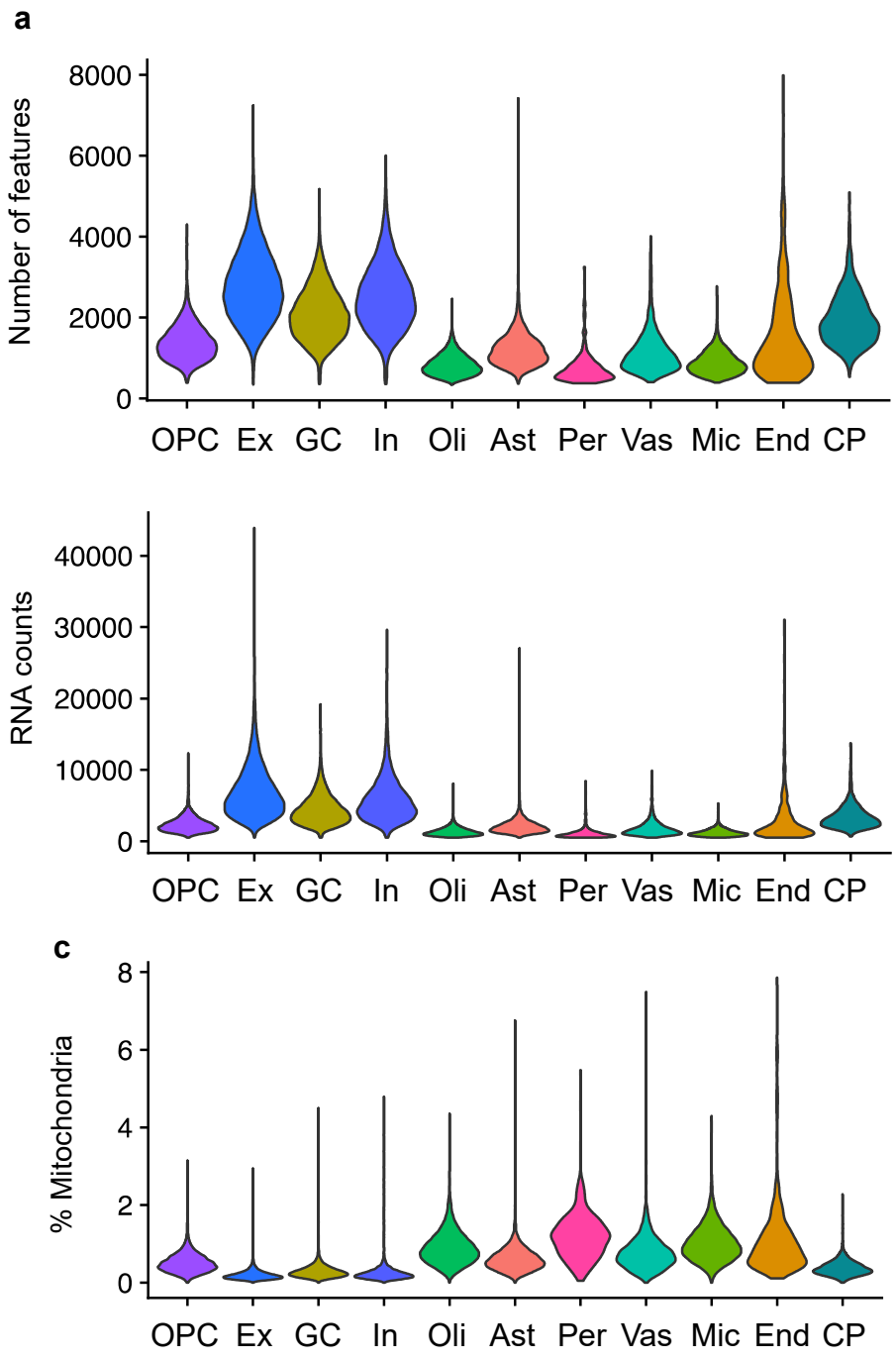

Supplementary Fig. 3. snRNA-seq coverage, depth, and quality control. a, Violin plots showing estimated nuclei counts and mean reads per nucleus per sample, based on Cell Ranger (v6.1.2) metrics_summary. **b**, Violin plots showing the distribution of detected features, RNA counts, and mitochondrial transcript percentages across all cell types. **c**, Violin plots displaying the number of analyzed genes/features (defined as expressed in >1% of the respective population) per major cell type. OPC, oligodendrocyte precursor cells; Ex, excitatory neurons; GC, granule cells; In, inhibitory neurons; Oli, oligodendrocytes; Ast, astrocytes; Per, pericytes; Vas, vascular and leptomeningeal cells; Mic, microglia; End, endothelial cells; CP, choroid plexus cells.

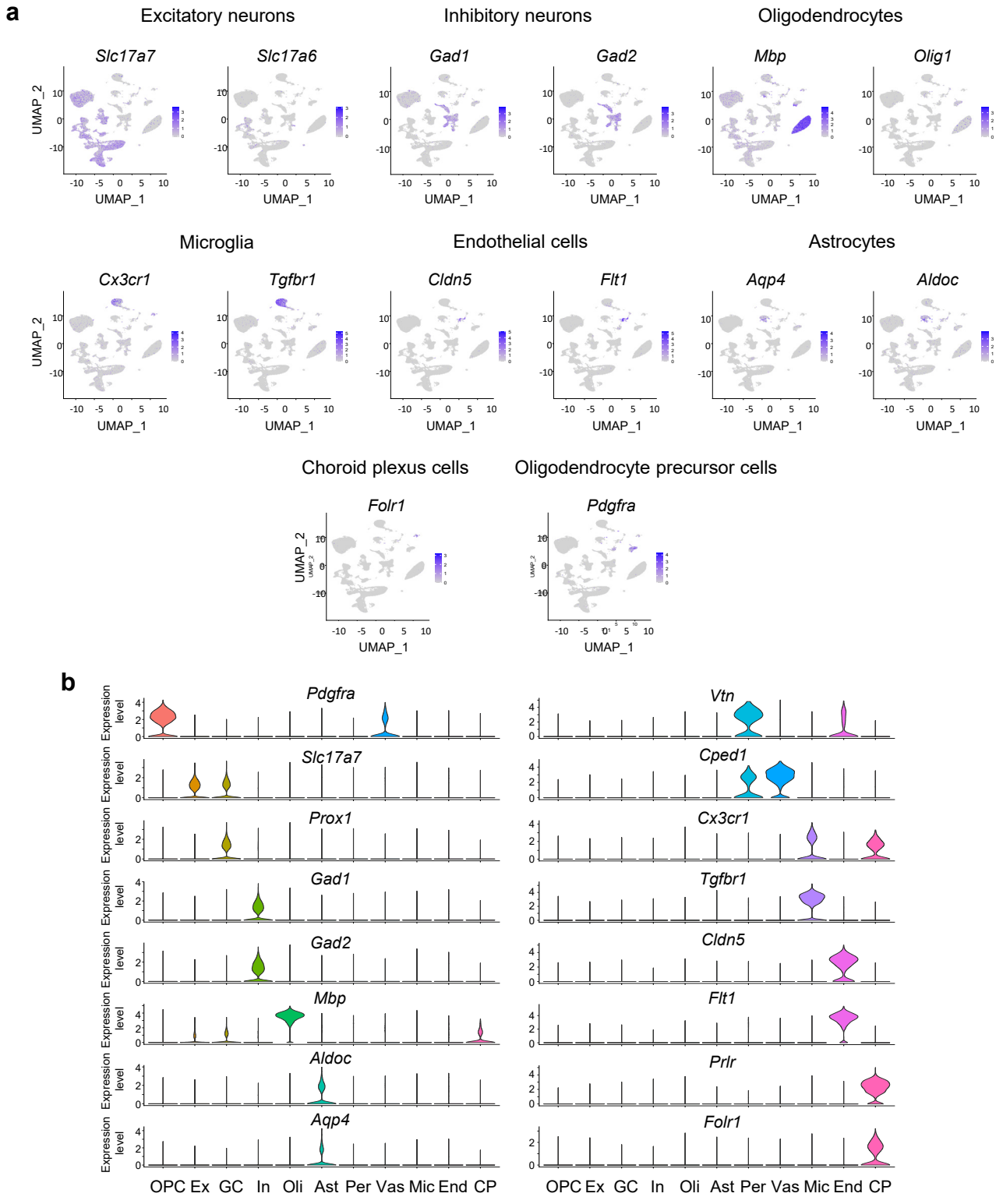

Supplementary Fig. 4. Cell type-specific marker expression in hippocampal snRNA-seq from 3xTg mice. a, UMAP feature plots showing the expression of established cell type-specific markers across cells types from the snRNA-seq experiment. **b**, Violin plots displaying the relative expression of cell type-specific markers in the designated cell types. OPC, oligodendrocyte precursor cells; Ex, excitatory neurons; GC, granule cells; In, inhibitory neurons; Oli, oligodendrocytes; Ast, astrocytes; Per, pericytes; Vas, vascular and leptomeningeal cells; Mic, microglia; End, endothelial cells; CP, choroid plexus cells.

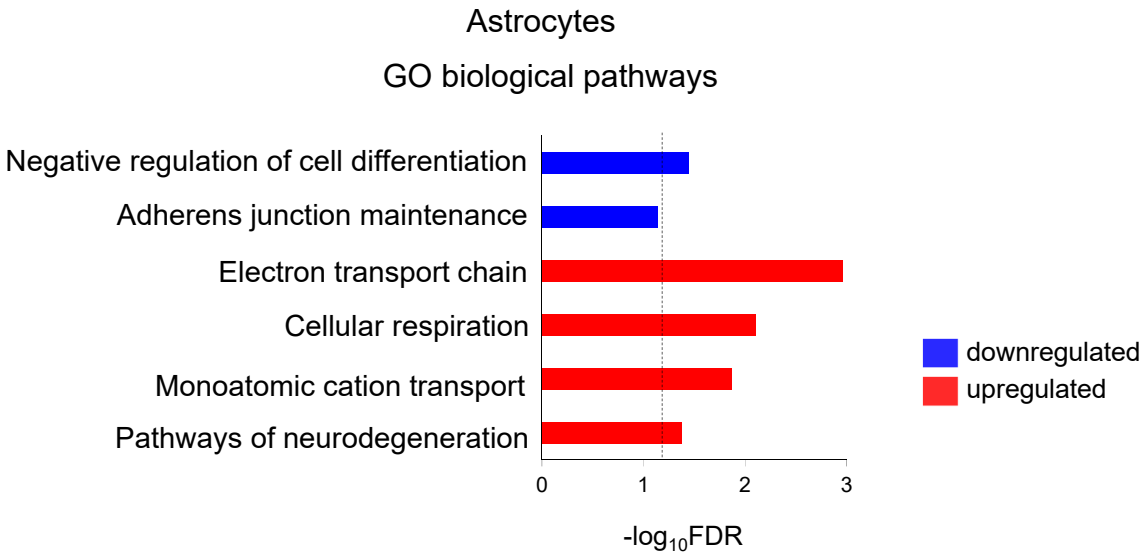

Supplementary Fig. 5. GO analysis of DEGs in lithium-deficient 3xTg astrocytes. GO pathway enrichment analysis was performed on differentially expressed genes identified by snRNA-seq in hippocampal astrocytes from 12-month-old 3xTg mice fed a Li-deficient (DEF, n=5) or control (CTRL, n=4) diet for 5 weeks. Pathways enriched among downregulated (blue) and upregulated (red) genes are shown.

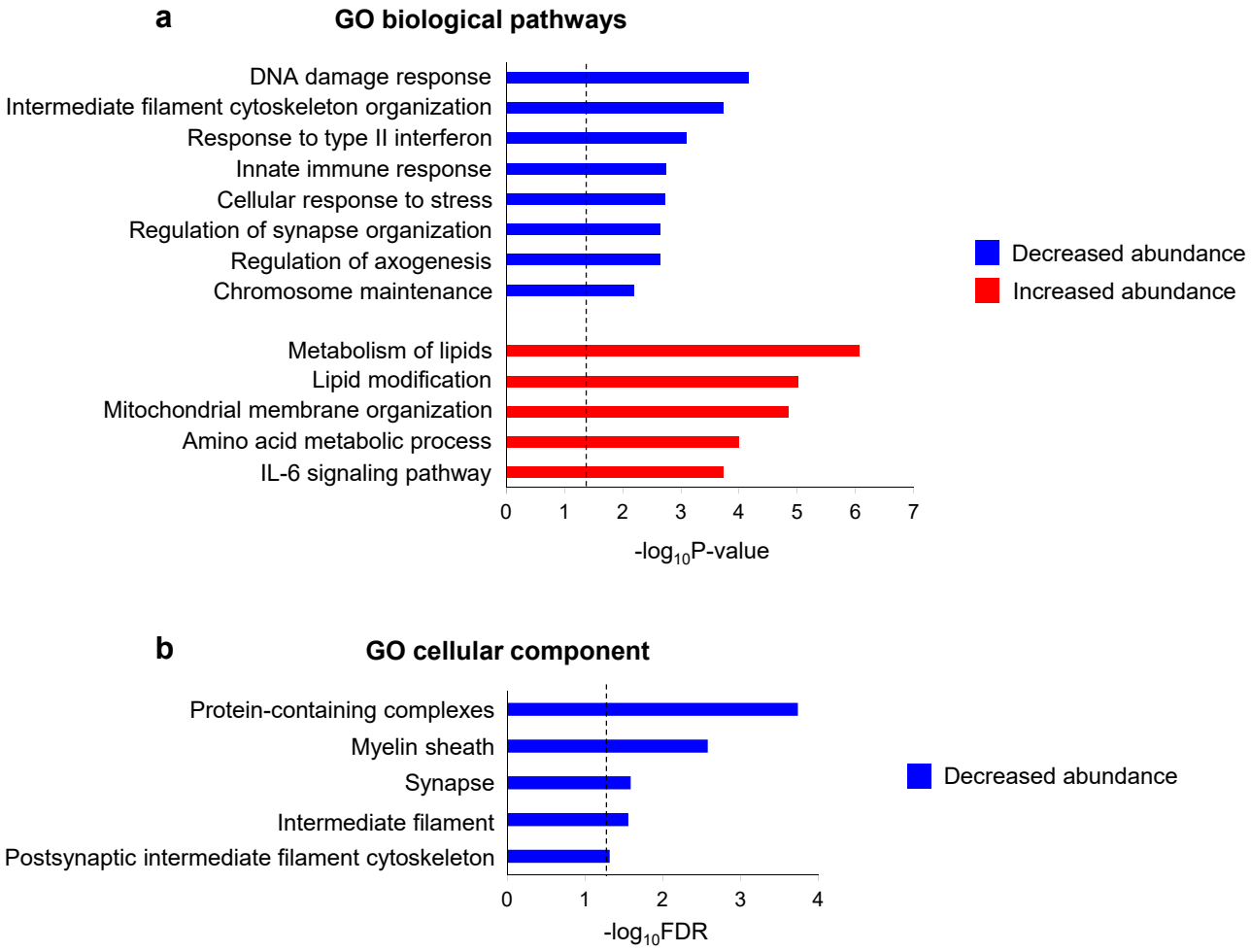

Supplementary Fig. 6. Mass spectrometry analysis of the hippocampus in lithium-deficient 3xTg mice. a, GO analysis of biological pathways enriched among proteins with increased (red) or decreased (blue) abundance in the hippocampus of Li-deficient versus control 3xTg mice. **b**, GO analysis of cellular components significantly enriched among proteins with decreased abundance. No significant enrichment was observed among proteins with increased abundance. Mass spectrometry was performed on hippocampal tissue from 15-month-old 3xTg mice maintained on a Li-deficient (n=4) or control (n=4) diet from 6-15 months of age. See Supplementary Table 7 for the full protein list and GO enrichment terms.

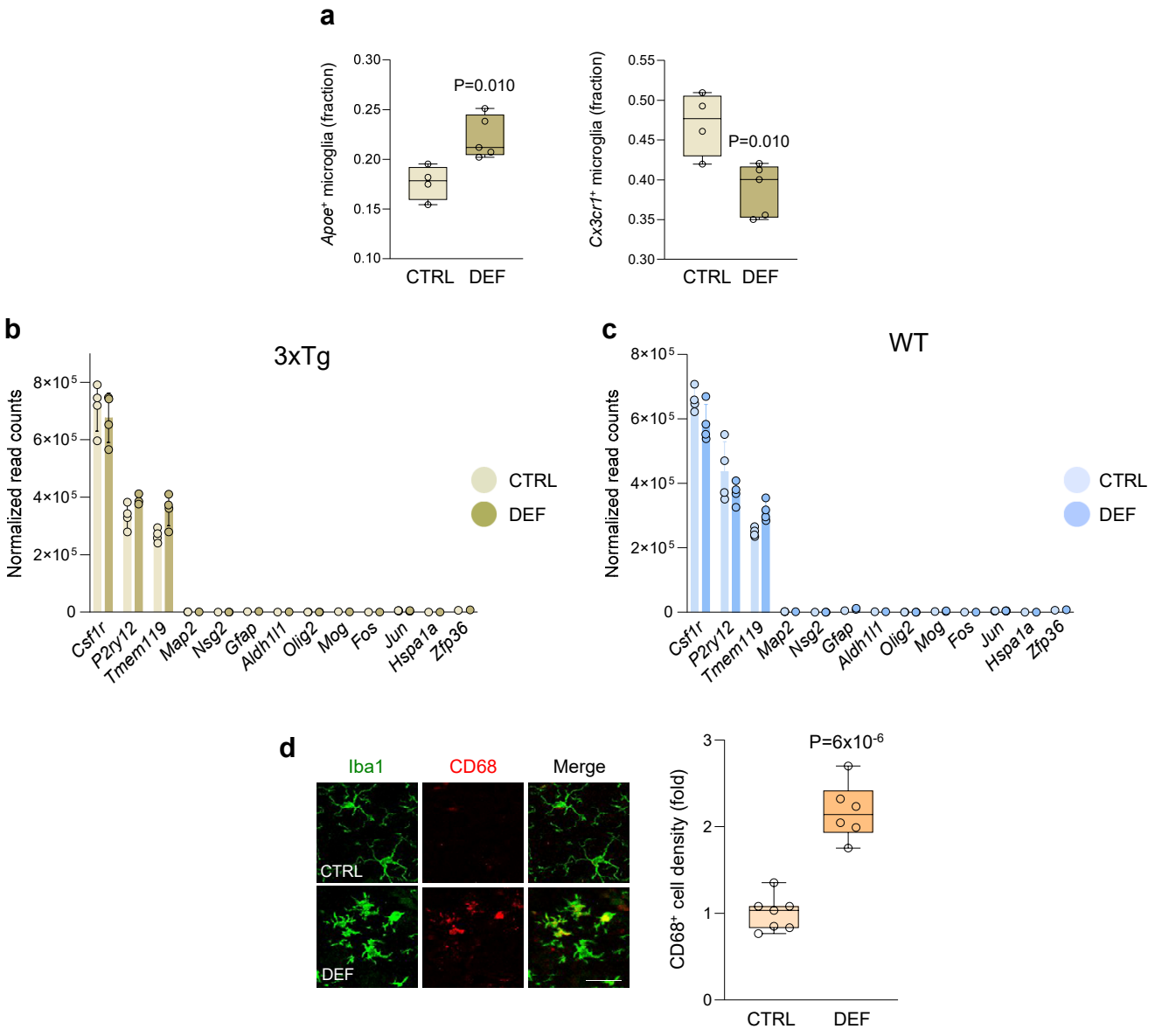

Supplementary Fig. 7. Characterization of microglia from Li-deficient mice. a, Reduced number of homeostatic *Cx3cr1*-expressing and increased number of reactive *Apoe*-expressing microglia in Li-deficient (DEF) mice. Values were derived from snRNA-seq in 3xTg mice on DEF (n=5) or control (CTRL, n=4) diets. **b**,**c**, Purity of isolated microglia from Li-deficient and control 3xTg (**b**) and WT (**c**) mice. Expression of microglial (*Csf1r*, *P2ry12*, *Tmem119*), neuronal (*Map2*, *Nsg2*), astrocytic (*Gfap*, *Aldh1l1*), and oligodendrocyte (*Olig2*, *Mog*) marker genes, as well as markers of ex-vivo microglia activation (*Fos*, *Jun*, *Hspa1a* and *Zfp36*) were determined (n=4 mice/group). Note the selective expression of microglial genes and the absence of gene expression previously associated with ex-vivo microglial manipulation and stress[16]. **d**, Immunolabeling of activated microglia ($CD68^+$) and all microglia ($Iba1^+$) in the hippocampus of 6-month-old J20 mice administered the CTRL (n=7) or DEF (n=6) diets from 3-6 months of age, and quantification (right) of $CD68^+$ cell density. The data was normalized to the mean of the CTRL group. Scale bar, 25 µm. **a**,**d**, Box plots show individual values, median (line), box limits (25^{th}-75^{th} percentiles), and whiskers (min-max). **b**,**c**, Shown are individual values, as well as means ± s.e.m. **a**-**d**, P-values by two-tailed, unpaired t-tests. **b**,**c**, *P*-values can be found in the Source Data file.

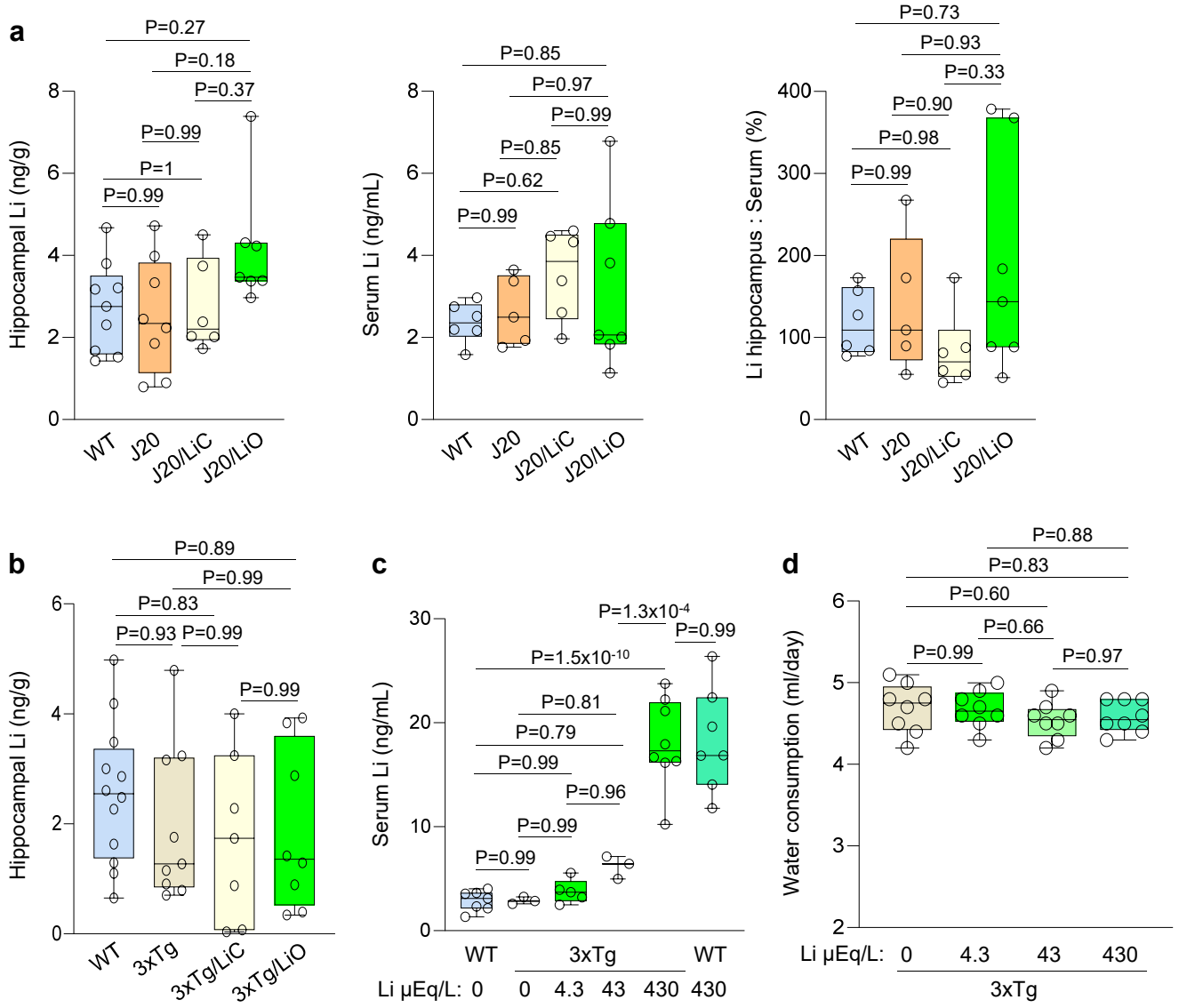

Supplementary Fig. 8. Measurement of Li levels in in J20 and 3xTg mice following administration of lithium salts. a,b, Total hippocampal Li (**a**, left; b), serum Li (**a**, middle) and ratio of hippocampus-to-serum Li (**a**, right) were assessed in 18-month-old J20 (**a**) or 3xTg (**b**) mice after treatment with the indicated Li salts or vehicle (water) for 7 days. **c**, Serum Li levels in 3xTg and WT mice treated with LiO (4.3-430 µEq/L) or vehicle (water) from 5-12 months of age. **d**, Daily water consumption for 3xTg mice that were administered LiO (4.3-430 µEq/L) in the drinking water. Box plots show individual values, median (line), box limits (25^{th}-75^{th} percentiles), and whiskers (min-max). P-values were determined by one-way (**d**) or two-way (**a**-**c**) ANOVA followed by Tukey's post-hoc test. In **a**, left WT n=9, J20 n=8, J20/LiC n=6, J20/LiO n=7. In **a**, middle and right WT n=6, J20 n=5, J20/LiC n=6, J20/LiO n=7. In **b**, WT n=12, 3xTg n=9, 3xTg/LiC n=7, 3xTg LiO n=8. In **c**, WT n=7, 3xTg n=3, 3xTg/LiO 4.3 n=5, 3xTg/LiO 43 n=3, 3xTg/LiO 430 n=8, WT/LiO 430 n=7. In **d**, n=8 mice per group.

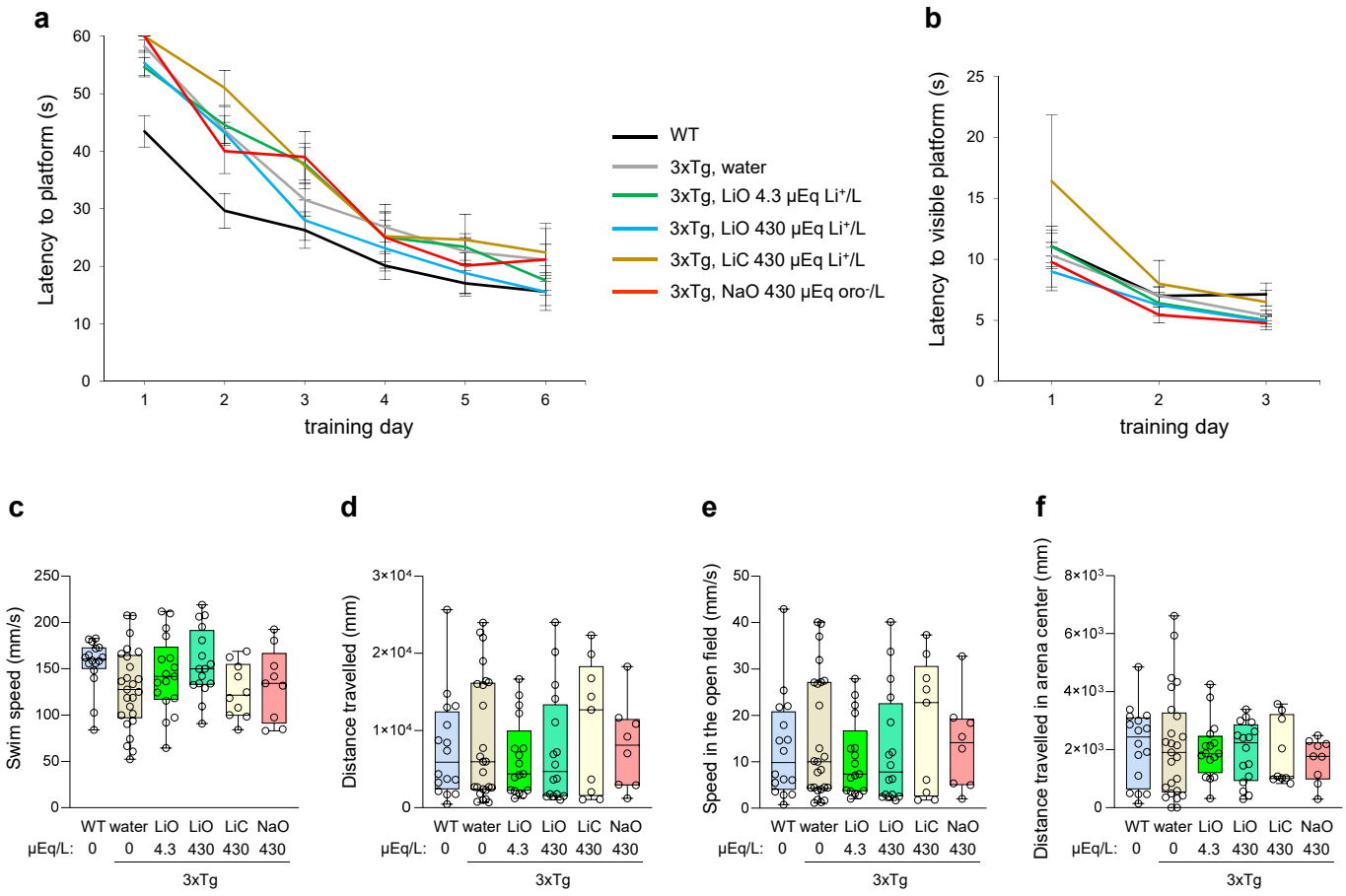

Supplementary Fig. 9. Administration of LiO does not alter exploratory, visual and motor parameters in 3xTg mice. Behavioral analysis of 3xTg mice administered LiO, LiC, NaO or vehicle from 5-12 months of age. **a**, Latency to reach the hidden platform during Morris water maze training. **b**-**f**, No significant differences were seen in latency to reach a visible platform (**b**) or swim speed (**c**) in the Morris water maze, or activity in the open field arena (**d**-**f**). WT n=16; 3xTg/water n=25; 3xTg/LiO 4.3 n=17 (**a**-**e**), n=16 (**f**); 3xTg/LiO 430 n=16; 3xTg/LiC 430 n=10 (**a**-**c**), n=9 (**d**-**f**); 3xTg/NaO 430 n=9. **a**,**b,** Data was analyzed using mixed-effects models with repeated measures, followed by Tukey's post-hoc test. **c**-**f**, The data was analyzed by one-way ANOVA with Tukey's post-hoc test. No significant differences between any groups were detected. Adjusted *P*-values can be found in Source Data file. Data are represented as means ± S.E.M (**a**,**b**) or box plots with individual values, median (line), box limits (25^{th}-75^{th} percentiles), and whiskers (min-max) (**c**-**f**).

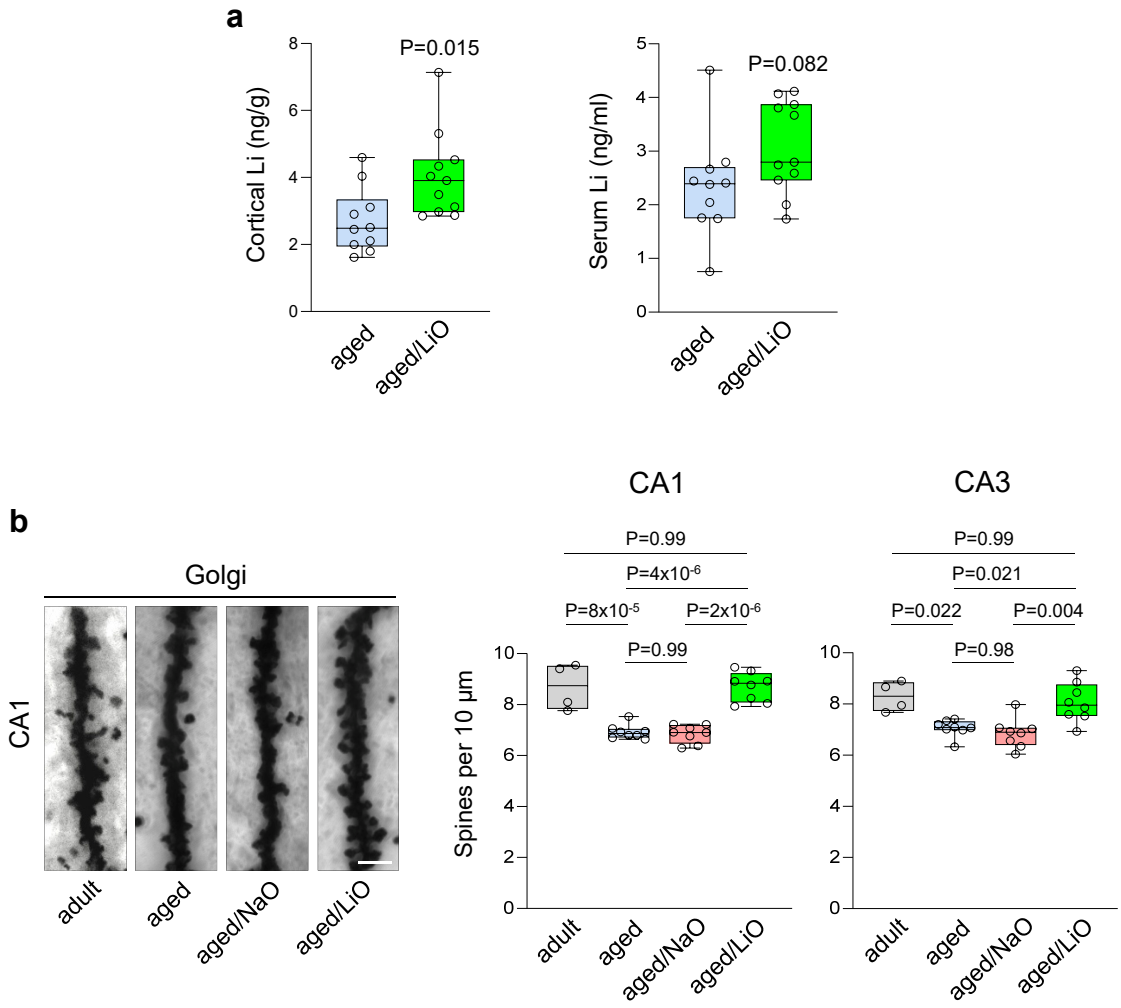

Supplementary Fig. 10. Lithium and cognitive resilience during aging. a, Low dose LiO (4.3 µEq/L) modestly elevates cortical and serum Li levels in aging WT mice (n=10 water, n=11 LiO). **b**, LiO prevents age-related dendritic spine loss in WT mice. Left panel: Golgi labeling of dendritic spines in CA1 hippocampal neurons of young adult 3-month-old WT mice (adult), or 20-month-old WT mice administered LiO (4.3 µEq/L), NaO (4.3 µEq/L), or vehicle from 12-20 months of age. Middle and right panels: Quantification of dendritic spine density in CA1 (middle) and CA3 (right) hippocampal neurons. n=4 mice for adult, and n=8 per group for aged mice. Box plots show individual values, median (line), box limits (25^{th}-75^{th} percentiles), and whiskers (min-max). P-values by the two-tailed unpaired t-test (**a**) or two-way ANOVA with Tukey's post-hoc test (**b**). Scale bar, 5 µm.

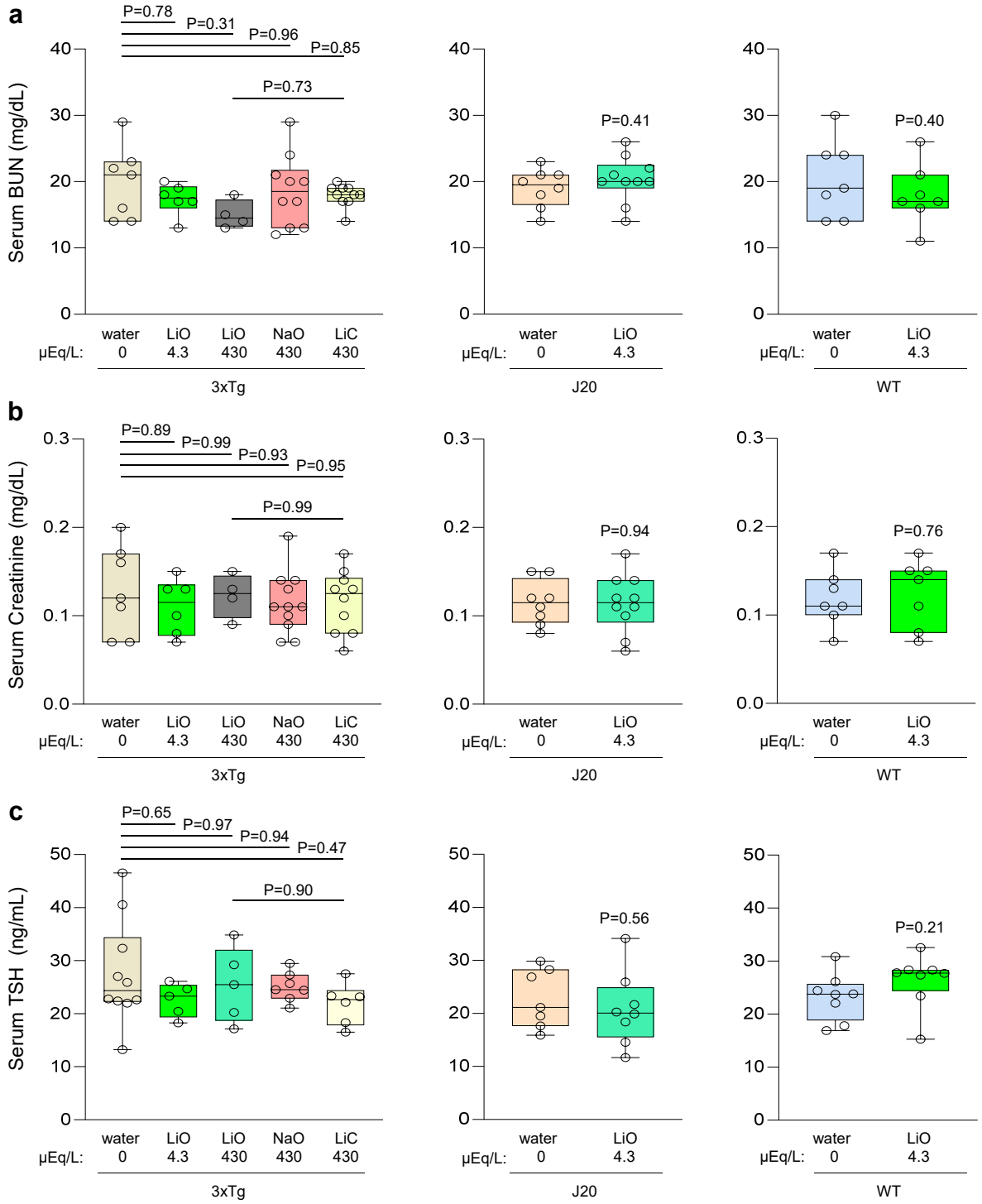

Supplementary Fig. 11. Absence of kidney or thyroid toxicity after chronic treatment with lithium orotate. **a**, Serum blood urea nitrogen (BUN). **b**, Serum Creatinine. **c**, Serum thyroid-stimulating hormone (TSH). Serum levels were measured in three independent cohorts of mice: (i) 3xTg mice administered LiO (4.3 or 430 μEq Li/L), LiC (430 μEq Li/L), Na orotate (430 μEq/L) or vehicle (water) from 5-12 months of age; (ii) J20 mice administered LiO (4.3 μEq Li/L) or vehicle from 17-22 months of age; and (iii) WT mice administered LiO (4.3 μEq Li/L) or vehicle from 12-24 months of age. Box plots show individual values, median (line), box limits (25^{th}-75^{th} percentiles), and whiskers (min-max). *P*-values by one-way ANOVA with Tukey's post-hoc test (left panels) or two-tailed unpaired t-test (middle and right panels). In **a**,**b**, left panels: water n=7; LiO 4.3 n=6; LiO 430 n=4; NaO n=10 (**a**), n=11 (**b**); LiC n=10. In **c**, left panel: water n=10, LiO 4.3 n=5, LiO 430 n=5, NaO n=7, LiC n=6. In **a**-**c**, middle panels, water n=8 (**a**,**b**), n=7 (**c**); LiO n=10 (**a**,**b**), n=8 (**c**). In **a**-**c**, right panels: water n=7 (**a**,**b**), n=8 (**c**); LiO n=7 (**a**,**b**), n=8 (**c**).